Received May 1, 2018, accepted May 23, 2018, date of publication May 28, 2018, date of current version July 12, 2018.

Digital Object Identifier 10.1109/ACCESS.2018.2841194

HICIC: Hybrid Inter-Cell Interference Coordination for Two-Tier Heterogeneous Networks With Non-Uniform Topologies

JINJING HUANG, JIANDONG LI, (Senior Member, IEEE), ZICHEN CHEN, AND HAO PAN

State Key Laboratory of Integrated Service Networks, Xidian University, Xi'an 710071, China

Corresponding author: Jiandong Li (jdli@ieee.org)

This work was supported by the Key Program of the National Natural Science Foundation of China under Grant 91638202 and Grant 61231008.

ABSTRACT Interference coordination is regarded as one of the most significant techniques in heterogeneous networks (HetNets). In this paper, we propose a novel interference coordination framework, which is referred to hybrid inter-cell interference coordination (HICIC), for interference mitigation in HetNets with non-uniform topologies. The meaning of hybrid is two-fold: first, several techniques belong to inter-cell interference coordination (ICIC), enhanced ICIC (eICIC), and further eICIC (FeICIC) are considered simultaneously. We perform the resource partition in both the time-domain and the frequency-domain jointly. A novel dummy base station structure is designed to take full advantage of resources. Second, different subbands in the same cell can be configured with different almost blank subframe (ABS) ratios for diverse purposes. A novel concept, coordination willingness, is proposed for determining ABS ratios in a distributed manner with limited signaling overhead. We formulate HICIC parameters optimization as a logarithm utility maximization problem and provide a semi-distributed algorithm comprising three stages to solve it. Numerical results demonstrate the efficiency of HICIC over several comparative schemes in HetNets with two different non-uniform topologies. It achieves the maximal system utility among all schemes and improves the performance of user equipment's (UEs) who have geographical disadvantages. With HICIC, sum throughput of all UEs has a significant increase with slight losses in the fairness. Our work also verifies the fact that ICIC and eICIC/FeICIC are not either-or propositions. A reasonable combination of different techniques can mitigate interference effectively making a better HetNet.

INDEX TERMS Almost blank subframe, heterogeneous networks, interference coordination, LTE, multi-cell network, user association, non-uniform topology.

I. INTRODUCTION

With the explosive growth of mobile data traffic, heterogeneous networks (HetNets) are believed to be the centerpiece of utilizing the available radio spectrum in an effective and cost-efficient way to realize ever-increasing network capacity. In a HetNet architecture, the footprint of a usual macro base station (MBS) is overlaid with several low-powered access nodes, such as pico base stations (PBSs), femto base stations (FBSs), and relays [1]. PBSs attract considerable attention because they are typically operator-deployed and open access to all user equipments (UEs). The transmission power of MBSs is much larger than that of PBSs which presents both opportunities for cell splitting gain and challenges for network design and optimization. Inter-cell interference (ICI) limits the system performance, especially for UEs near cell boundaries.

Inter-cell interference coordination (ICIC) is seen as an efficient approach to alleviate ICI by applying restrictions on the allocation of various system resources. After ICIC is initially mentioned in [2], several schemes for mitigating inter-cell interference among MBSs are proposed by Huawei [3], Ericsson [4], Siemens [5], and etc. Each of them is a network-wide agreement that all MBSs in the network must be subject to their predefined frequency resource partitioning patterns. A survey of ICIC techniques is presented in [6] for different mobile scenarios recently. Deployment of HetNets has further complicated the problem brought by ICI. 3GPP presents a set of techniques named enhanced ICIC

(eICIC) to resolve this problem since release-10 [7]. Two representative techniques are described briefly below.

- Cell range expansion (CRE) is realized by applying nonnegative biases on reference signal received power (RSRP) of PBSs to offload UEs. However, downlink transmissions of PBSs suffer strong cross-tier interference from surrounding MBSs, especially for the offloaded UEs by CRE.
- Almost blank subframe (ABS) is configured in MBSs that they should inhibit data transmissions in some subframes, while pilot signals must be transmitted all the time. Utilization of ABS can reduce the interference from MBSs to PBSs, but this is realized at the price of the performance of UEs associated with MBSs.

Moderate interference is permissible since automatic modulation and coding (AMC) is adopted in LTE/LTE-A HetNets. Further eICIC (FeICIC) with low-power ABS (LP-ABS) is proposed in 3GPP release-11 [8] intended to replace the previous zero-power ABS (ZP-ABS). MBSs recover transmission opportunities for UEs near them in ABSs of FeICIC with some power limitations. Obviously, ZP-ABS is a special case of LP-ABS.

Researchers have paid much attention to eICIC/FeICIC design and optimization in the literature available. Qualcomm presents some initial simulation results for reference [9]. In [10], the performance of a HetNet with static eICIC is analyzed with varying parameters, such as the number of PBSs, transmission power, and UEs distribution. Pang *et al.* [11] present a distributed method with more detailed UEs classification to optimize the ABS ratio. The ABS ratio and the bias for CRE are optimized independently in [12] by a self-optimizing algorithm. Dual decomposition is utilized to optimize UE association and ABS configuration jointly in [13], while Zhou *et al.* [14] tackle the same problem by alternating direction method of multipliers (ADMM) to accelerate calculations. Considering quality of service (QoS) requirements, a distributed scheme similar to [13] is designed by dividing the system bandwidth into two subbands in [15]. One of the subbands is reserved for PBSs exclusively. Some references consider both the time-domain and the frequency-domain jointly. Liu *et al.* [16] design a two-timescale hierarchical method to select almost blank resource blocks (ABRBs) dynamically while not the ABS ratio. Pao *et al.* [17] design a joint time-frequency allocation scheme and evaluation functions for ABS ratio determination and UE grouping. Nevertheless, both of these references have ZP-ABS or zero power subband setting for MBSs and this is a waste of resource. Song *et al.* [18] propose a distributed interference coordination algorithm by power control and UEs classification. Note that energy efficiency is another important metric [19], eICIC and FeICIC are concerned again recently. Virdis *et al.* [20] consider ZP-ABS and LP-ABS simultaneously and design a distributed framework from the standpoint of power saving. In [21], a distributed algorithm based on potential game is presented for FeICIC optimization in which both spectral efficiency and energy efficiency are taken into account.

Most studies on the time-domain eICIC/FeICIC neglect the effect of ICIC in the frequency-domain, and vice versa. The relationship of ICIC and eICIC has been discussed in [13] and the authors claim that these two technologies are not either-or propositions. Both ICIC and eICIC/FeICIC are aimed to improve the performance of UEs near cell boundaries. It is of importance to note that the cell boundary is redefined in a HetNet because each PBS has its own cell border. These technologies can be combined to reach the goal. UEs located near PBSs can benefit from ICIC or eICIC, while UEs who have no candidate PBSs to associate must call for help from ICIC. Additionally, synchronous ABS configuration is preferred in the literature because the spectrum reuse gain decreases under asynchronous configuration [11]. Nevertheless, the number of UEs varies in the footprint of MBSs, so does that of PBSs. This results in a HetNet with non-uniform topology and the strict synchronous ABS configuration is no longer appropriate. In [22], optimizations of UE association, ABS configuration, and transmission power in ABS subframes are conducted alternately for a HetNet with non-uniform topology, while it may be trapped in some local optimal solutions, such as ZP-ABS. This is because the optimization problem is neither convex nor concave with respect to the transmission power of MBSs [23]. Additionally, Peng *et al.* [24] try to deploy ultra-dense heterogeneous relay networks for non-uniform hotspots.

Motivated by observations above, we propose the hybrid inter-cell interference coordination (HICIC) to mitigate interference in HetNets with non-uniform topologies. The meaning of hybrid is two-fold: firstly, it utilizes technologies belong to ICIC and eICIC/FeICIC jointly to deal with interference at the same time. Parameters of eICIC/FeICIC are adjusted based on the frequency division of ICIC. And secondly, different subbands of an MBS can be configured with different ABS ratios that HICIC is actually a semi-synchronous method. Although there is no UEs classification which is a basic operation in traditional ICIC schemes, HICIC can inherit the conciseness and efficiency of the standard soft frequency reuse (SFR). Our contributions are listed below:

- To take full advantage of resources, we propose a novel dummy base station (BS) structure in which resources in an ABS period are resembled. All available resource blocks (RBs) of an MBS are partitioned in both the frequency-domain and the time-domain. RBs with full transmission power are separated from those with constrained transmission power so that two dummy BSs are constructed in an MBS.
- A simple but efficient coordination mechanism is designed to determine ABS ratios for MBSs. A novel concept, coordination willingness, is defined by taking into consideration both the selfish desire of a cell and requirements of its neighbors.
- To determine UE associations, we propose a centralized UE association method. The method is mainly based on

the work in [25], while some necessary modifications are conducted to enhance the robustness. A termination rule considering the oblivious integrality gap is adopted in our proposed method.

- HICIC is compared with other schemes under two different non-uniform topologies, a simple one and a complex one. Numerical results demonstrate that HICIC can achieve the maximal system utility among all schemes. Sum throughput of all UEs has a significant increase with slight losses in fairness. It also improves the performance of UEs who have geographical disadvantages. In addition, we analyze the convergence property of the UE association algorithm and the effect of transmission power reduction ratios by simulation.

The remainder of this paper is organized as follows. Section II describes our system model and some necessary assumptions. In Section III, we formulate HICIC parameters optimization as a logarithm utility maximization problem and discuss its hardness. A semi-distributed algorithm comprising three stages is designed in Section IV. We present numerical results and analysis in Section V. Finally, our work is concluded in Section VI.

II. SYSTEM MODEL

A. NETWORK MODEL

We consider the downlink of a two-tier HetNet. It consists of multiple MBSs, denoted by $\mathcal{M} = \{1, 2, \ldots, m, \ldots M\}$, overlaid with several PBSs, denoted by $\mathcal{P} = \{1, 2, \ldots, p, \ldots P\}$. Each PBS is equipped with an omni-directional antenna, while each MBS has a directional transmit antenna with 120° beamwidth (3dB beamwidth of 65°) so that MBS m covers cell m.We provide a simple two-tier HetNet and an enlarged view of the part of three MBSs sharing the same cell site for illustration in Fig. 1.

Remark 1: In general, there is only one MBS at a cell site and three directional transmit antennas are installed at an MBS resulting three hexagonal sectors. Since different resource partition patterns are prepared for different sectors, we assume that there are three MBSs at a cell site and each MBS is equipped with only one directional transmit antenna. The concept ''sector'' is replaced with ''cell'' to address this assumption.

The set of PBSs that located in cell m is denoted by $\mathcal{P}_m$. The set of MBSs who have strong interference to PBS p is denoted by $\mathcal{I}_p \in \mathcal{M}$. $\mathcal{I}_p$ can be constructed either by cell-adjacency relationship or based on whether or not the RSRP of an MBS at PBS p is greater than a predefined threshold P_{th} [13]. In this paper, we select the latter one and define two important sets of MBSs below.

1) COORDINATION NEIGHBOR LIST

$\mathcal{CL}_m$ is the coordination neighbor list of MBS m containing indexes of MBSs who have strong interference to PBSs belong to $\mathcal{P}_m$. It can be expressed explicitly as:

$$\mathcal{CL}_m = \bigcup_{p \in \mathcal{P}_m} \mathcal{I}_p, \quad \mathcal{CL}_m \subseteq \mathcal{M}. \tag{1}$$

Note that $m \in \mathcal{CL}_{m'}$ does not mean $m' \in \mathcal{CL}_m$.

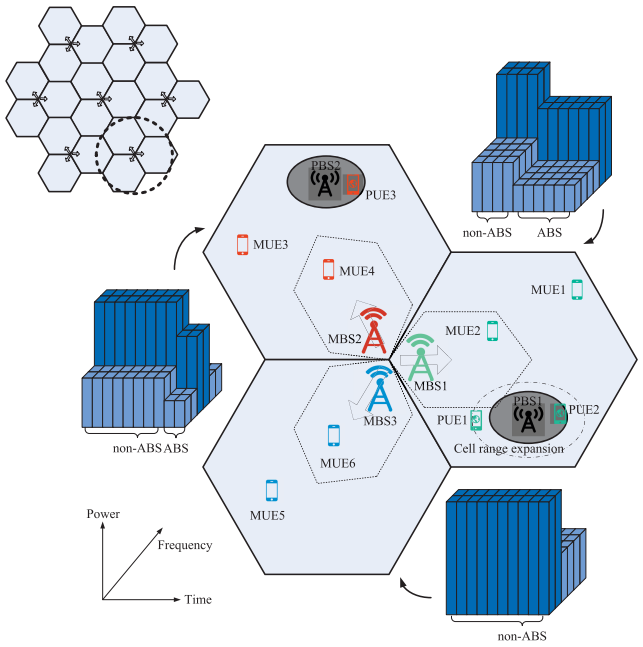

FIGURE 1. A simple two-tier HetNet.

2) REQUEST NEIGHBOR LIST

$\mathcal{RL}_m$ is the request neighbor list of cell m. It is related to coordination neighbor lists of neighboring MBSs and can be written as:

$$\mathcal{RL}_m = \left\{ m' \middle| \, m \in \mathcal{CL}_{m'}, m' \in \mathcal{M} \right\}. \tag{2}$$

B. RESOURCE MODEL

Our work aims at answering questions how to share radio resources available among MBSs and PBSs and how to associate UEs to base stations (BSs). The time scale of our work is more than several minutes, but a guide can be given for real-time scheduling in practice. Inspired by the discussion on the relationship of ICIC and eICIC in [13], we carry out resource partitioning in both the frequency-domain and the time-domain jointly.

In the frequency-domain, SFR is adopted because it can achieve a universal frequency reuse. As illustrated in the upper left part of Fig. 2, the total N_{sc} subchannels are combined into three subbands, namely B_1, B_2, and B_3. The bandwidth of subband B_X is W_X. In each cell, a subband is reserved as its major band transmitting with relatively higher power. Directly adjacent cells must keep their major bands orthogonal to each other. The other two subbands constitute the minor band on which the transmission power is restricted.

In the time-domain, ABS subframes are configured in MBSs. The ABS period is denoted by N_{sf} that is the total number of subframes over which ABS subframes are reserved. Indexes of subframes in an ABS period must be aligned across all MBSs and PBSs. The proportion of ABS subframes named ABS ratio, denoted by α, is actually a discrete value. ABS subframes are the last several contiguous subframes in an ABS period. We assume that each cell must reserve some RBs with relatively higher transmission power to guarantee the network coverage, so the ABS ratio is never to be 1. All possible values are summarized in the ABS ratio list:

$$\mathcal{AL} = \left\{\alpha \,|\, 0 \le \alpha < 1,\ \alpha N_{sf} \in \left\{0, 1, \ldots, N_{sf}-1\right\}\right\}. \quad (3)$$

Additionally, since the total frequency band has been divided into two parts previously, the ABS ratio of the major band, α^{E}, can be different with α^{C}, that of the minor band.

Remark 2: The reason why E represents the major band is that these resources are mostly applied to UEs located in the cell edge region of a homogeneous network composed by MBSs. Accordingly, C represents the minor band because UEs located in the cell center region are the most likely UEs.

Unless otherwise specified, we take an MBS who reserves subband B_3 as its major band for example. In the right part of Fig. 2, all available RBs of the MBS in an ABS period are divided as aforementioned. Obviously, the division creates four types of RBs:

- NC: non-ABS subframes, minor band;
- AC: ABS subframes, minor band;
- NE: non-ABS subframes, major band;
- AE: ABS subframes, major band.

The transmission power of an RB is determined according to its type:

$$\begin{cases} P^{\mathrm{NE}} = P_{total}/N_{sc}, \\ P^{\mathrm{NC}} = \beta^{\mathrm{NC}} P^{\mathrm{NE}}, \\ P^{\mathrm{AE}} = \beta^{\mathrm{AE}} P^{\mathrm{NE}}, \\ P^{\mathrm{AC}} = \beta^{\mathrm{AC}} P^{\mathrm{NE}}, \end{cases} \quad (4)$$

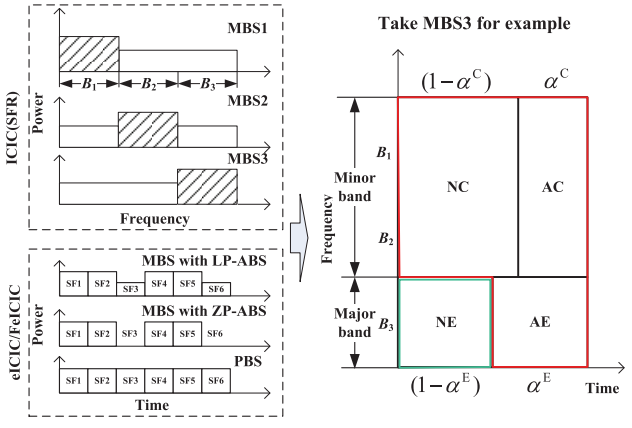

FIGURE 2. Two dimensional resource partition illustration.

where β^{NC}, β^{AE}, and β^{AC} are relative power reduction ratios restricted in the interval from 0 to 1. Different types of RBs can be configured with different transmission power levels. It is indeed a multi-level LP-ABS scheme, even a mixture of ZP-ABS and LP-ABS. Although these ratios are adjustable parameters, fast power control is not considered in this paper. Assaad [26] claim that adaptive modulation coding is able to cope with fast variations of radio channels. Furthermore, fast power control will result in interference fluctuation. We will analyze the effect of these parameters by simulation in Section V.

With the resource partition and the transmission power differentiation above, we can visualize each MBS as two dummy base stations. The high power dummy BS (HPD) only has exclusive access to RBs in NE. The set of all HPDs is denoted by $\mathcal{M}_{\mathrm{HPD}}$. The low power dummy BS (LPD) possesses RBs in NC, AE, and AC. $\mathcal{M}_{\mathrm{LPD}}$ is the set of all LPDs. LPD will provide services to UEs near the MBS. As shown in Fig. 1, UEs close to MBSs, such as those located within the smaller hexagons with dashed borders, can be associated with an LPD. For simplicity, we will refer to each of these as BS rather than dummy BS. Therefore, we have $2M + P$ BSs in the system. Let $\mathcal{B} = \mathcal{M}_{\mathrm{HPD}} \cup \mathcal{M}_{\mathrm{LPD}} \cup \mathcal{P}$ be the collection of all BSs in the HetNet.

C. USER MODEL

We assume UEs are pedestrians, and $\mathcal{U}$ is the set of all UEs in the system. The set of UEs located in cell m is denoted by $\mathcal{U}_m$. Full buffer assumption is adopted that persistent data traffic is generated for each UE and that there is an infinitely backlogged queue.

UEs have different spectrum efficiencies on different types of RBs. Assume cell m reserves subband B_3 as its major band. As for UE u utilizing RBs from MBS m, signal-to-interference-plus-noise ratio (SINR) expressions (5) and (6) with RBs in NE and AE are written explicitly as shown at the top of the next page:

where $P_{m'}^{NB_3}$ equals $P_{m'}^{\mathrm{NC}}$ or $P_{m'}^{\mathrm{NE}}$ depending on the identity of subband B_3 in MBS m', so do $P_{m'}^{AB_3}$. g_{um} and g_{up} are the channel gain between MBS m and UE u and the channel gain between PBS p and UE u, respectively. N_0 denotes the additive white Gaussian noise power. $Pr_{mm'}^{\mathrm{AB}_3}$ is the collision probability of subband B_3 between MBS m and m' in an ABS subframe, while $Pr_{mm'}^{\mathrm{NB}_3}$ is that in a regular subframe. Each PBS has no any ABS subframes, so the interference from a PBS is fixed. Nevertheless, interference from an MBS is weighted by values related to the corresponding collision probability. $Pr_{mm'}^{\mathrm{AB}_3}$ and $Pr_{mm'}^{\mathrm{NB}_3}$ can be evaluated by [27]:

$$Pr_{mm'}^{\mathrm{AB}_3} = \frac{\max\left(0, \alpha_m^{B_3} - \alpha_{m'}^{B_3}\right)}{\alpha_m^{B_3}}, \quad (7)$$

$$Pr_{mm'}^{\mathrm{NB}_3} = \frac{1 - \max\left(\alpha_m^{B_3}, \alpha_{m'}^{B_3}\right)}{1 - \alpha_m^{B_3}}, \quad (8)$$

$$\mathrm{SINR}_{um}^{\mathrm{NE}} = \frac{P^{\mathrm{NE}} g_{um}}{\sum\limits_{\substack{m' \neq m \\ m' \in \mathcal{M}}} \left(P_{m'}^{\mathrm{NB}_3} Pr_{mm'}^{\mathrm{NB}_3} + P_{m'}^{\mathrm{AB}_3} \left(1 - Pr_{mm'}^{\mathrm{NB}_3} \right) \right) g_{um'} + \sum\limits_{p \in \mathcal{P}} P_p g_{up} + N_0}, \tag{5}$$

$$\mathrm{SINR}_{um}^{\mathrm{AE}} = \frac{P^{\mathrm{AE}} g_{um}}{\sum\limits_{\substack{m' \neq m \\ m' \in \mathcal{M}}} \left(P_{m'}^{\mathrm{NB}_3} Pr_{mm'}^{\mathrm{AB}_3} + P_{m'}^{\mathrm{AB}_3} \left(1 - Pr_{mm'}^{\mathrm{AB}_3} \right) \right) g_{um'} + \sum\limits_{p \in \mathcal{P}} P_p g_{up} + N_0}, \tag{6}$$

where $\alpha_m^{B_3} = \alpha_m^{\mathrm{E}}$ if B_3 is the major band of cell m, $\alpha_m^{B_3} = \alpha_m^{\mathrm{C}}$ otherwise. If the ABS ratio $\alpha_m^{B_3}$ equals 0, we calculate the SINR of an RB in NE with corresponding ABS ratios of interfering MBSs directly by the following equation:

$$\mathrm{SINR}_{um}^{\mathrm{NE}} = \frac{P^{\mathrm{NE}} g_{um}}{\sum\limits_{\substack{m' \neq m \\ m' \in \mathcal{M}}} \left(P_{m'}^{\mathrm{NB}_3} \left(1 - \alpha_{m'}^{B_3} \right) + P_{m'}^{\mathrm{AB}_3} \alpha_{m'}^{B_3} \right) g_{um'} + \sum\limits_{p \in \mathcal{P}} P_p g_{up} + N_0}. \tag{9}$$

If UE u is connected to PBS p located in cell m, $\mathrm{SINR}_{up}^{\mathrm{NE}}$ and $\mathrm{SINR}_{up}^{\mathrm{AE}}$ for RBs in B_3 can be written (10) and (11), as shown at the top of the next page.

Although PBS p has no ABS subframes, we denote $\alpha_p^{B_3} = \alpha_m^{B_3}$ to calculate the collision probability where m is the MBS covering the cell that it is located. $\alpha_p^{B_3}$ is interpreted as the proportion of subframes that PBS p enjoys reduced interference from MBS m [27]. PBS p is in coordination with MBS m, so $Pr_{pm}^{\mathrm{AB}_3} = 0$ and $Pr_{pm}^{\mathrm{NB}_3} = 1$. Furthermore, SINR expressions for RBs in NC and AC can be easily obtained by referring to equations from (5) to (11). It is of great importance to note that SINR of RBs in the two subbands making up the minor band must be calculated separately.

After obtaining SINR, the spectrum efficiency can be estimated by

$$\eta = \log_2 \left(1 + \mathrm{SINR} / \Gamma \right), \tag{12}$$

where $\Gamma = -\ln(5 \times \mathrm{BER}) / 1.5$ is the SNR gap [28]. We use R_{ub} to denote the maximum achievable data rate for UE u when it is assigned all available RBs of BS b. Assume b is located in cell m, R_{ub} is evaluated in the following forms:

$$R_{ub} = \begin{cases} \text{for } b \in \mathcal{M}_{\mathrm{HPD}}: \\ (1 - \alpha_m^{\mathrm{E}}) \eta_{um}^{\mathrm{NB}_3} W_3, \\ \text{for } b \in \mathcal{M}_{\mathrm{LPD}}: \\ \alpha_m^{\mathrm{C}} (\eta_{um}^{\mathrm{AB}_1} W_1 + \eta_{um}^{\mathrm{AB}_2} W_2) + \alpha_m^{\mathrm{E}} \eta_{um}^{\mathrm{AB}_3} W_3 \\ + (1 - \alpha_m^{\mathrm{C}}) (\eta_{um}^{\mathrm{NB}_1} W_1 + \eta_{um}^{\mathrm{NB}_2} W_2), \\ \text{for } b \in \mathcal{P}: \\ \alpha_m^{\mathrm{C}} (\eta_{ub}^{\mathrm{AB}_1} W_1 + \eta_{ub}^{\mathrm{AB}_2} W_2) + \alpha_m^{\mathrm{E}} \eta_{ub}^{\mathrm{AB}_3} W_3 \\ + (1 - \alpha_m^{\mathrm{C}}) (\eta_{ub}^{\mathrm{NB}_1} W_1 + \eta_{ub}^{\mathrm{NB}_2} W_2) \\ + (1 - \alpha_m^{\mathrm{E}}) \eta_{ub}^{\mathrm{NB}_3} W_3. \end{cases} \tag{13}$$

For convenience, we provide the list of used symbols of this paper in Table 1.

TABLE 1. List of symbols used.

Notation	Description
$\mathcal{M}, \mathcal{P}, \mathcal{B}, \mathcal{U}$	Set of MBSs, PBSs, BSs, and UEs
m, p, b, u	Typical MBS, PBS, BS, and UE
$\mathcal{M}_{\mathrm{HPD}}$,$\mathcal{M}_{\mathrm{LPD}}$	Set of high, low power dummy BSs
$\mathcal{P}_m$, $\mathcal{U}_m$	Set of PBSs and UEs in cell m
$\mathcal{I}_p$	Set of MBSs interfere p heavily
$\mathcal{CL}_m$	Coordination neighbor list of cell m
$\mathcal{RL}_m$	Request neighbor list of cell m
N_{sf}	Number of subframes in an ABS period
N_{sc}	Number of subchannels
$\beta^{\mathrm{NC}}, \beta^{\mathrm{AE}}, \beta^{\mathrm{AC}}$	Relative power reduction ratio
B_1, B_2, B_3	Label of subbands
W_1, W_2, W_3	Bandwidth of subbands
Pr	Probability of collision
η	Spectrum efficiency
α_m^{d}	Desired ABS ratio of cell m
α_m^{E}, α_m^{C}	ABS ratio of cell m major, minor band
$\boldsymbol{\alpha}^{\mathrm{E}}$, $\boldsymbol{\alpha}^{\mathrm{C}}$	ABS ratio vectors of HetNet
ω_m	Coordination willingness of cell m
R_{ub}	Max. achievable data rate of UE u with b
r_u	Actual data rate of UE u
x_{ub}	UE ass. indicator of UE u with b
y_{ub}	Proportion of resources for link from b to u
$\boldsymbol{x}_m$, $\boldsymbol{x}$	UE ass. indicator vector of cell m, HetNet
L_b	Load of BS b
$\boldsymbol{L}_m$, $\boldsymbol{L}$	Load vector of BSs in cell m, HetNet
ν_b	Dual variable for BS b
$\boldsymbol{\nu}_m$	Dual variable vector for BSs in cell m
Δ	Error tolerance
t	Outer iteration counter
T	Number of outer iterations
$\lambda^{(t)}$,$\gamma^{(t)}$,$\epsilon^{(t)}$	Assistant variables for optimization
$\epsilon, \rho, \theta, \underline{\gamma}, \overline{\gamma}$	Constants for optimization
P_{th}	RSRP threshold to determine $\mathcal{I}_p$
ϕ	Inter-cell handover threshold
k	Window length, calculate average throughput
$\hat{u}_b(t)$	Selected UE to schedule in BS b at slot t
$I_{ub}(t)$	UE selection indicator of BS b at slot t
$r_u(t)$	Instant data rate of UE u at slot t
$\bar{r}_u(t)$	k-point moving average throughput of u at t

III. PROBLEM FORMULATION

In this section, we formulate HICIC parameters optimization as a utility maximization problem.

A. OPTIMIZATION OBJECT

We desire to maximize the system throughput and maintain some level of fairness among UEs meanwhile. The tried and tested logarithmic utility function is selected as the optimization object. UE u makes a contribution to the system utility,

$$\mathrm{SINR}_{up}^{\mathrm{NE}} = \frac{P_p g_{up}}{\sum\limits_{m' \in \mathcal{M}} \left(P_{m'}^{NB_3} Pr_{pm'}^{NB_3} + P_{m'}^{AB_3} \left(1 - Pr_{pm'}^{NB_3} \right) \right) g_{um'} + \sum\limits_{\substack{p' \neq p \\ p' \in \mathcal{P}}} P_{p'} g_{up'} + N_0}, \tag{10}$$

$$\mathrm{SINR}_{up}^{\mathrm{AE}} = \frac{P_p g_{up}}{\sum\limits_{m' \in \mathcal{M}} \left(P_{m'}^{NB_3} Pr_{pm'}^{AB_3} + P_{m'}^{AB_3} \left(1 - Pr_{pm'}^{AB_3} \right) \right) g_{um'} + \sum\limits_{\substack{p' \neq p \\ p' \in \mathcal{P}}} P_{p'} g_{up'} + N_0}. \tag{11}$$

namely $\mathrm{Util}(r_u) = \log(r_u)$, where r_u is the actual data rate of UE u. The optimization object is:

$$\sum_{u \in \mathcal{U}} \mathrm{Util}(r_u). \tag{14}$$

B. OPTIMIZATION VARIABLES

The essence of HICIC is to determine association relationships (x_{ub}, $\forall u \in \mathcal{U}$) and to compute ABS ratios of the major band and the minor band (α_m^{E} and α_m^{C}, $\forall m \in \mathcal{M}$). The binary variable x_{ub} is the association indicator for UE u defined as follows:

$$x_{ub} = \begin{cases} 1, & u \text{ is associated with } b \in \mathcal{B}, \\ 0, & \text{otherwise.} \end{cases} \tag{15}$$

The ABS ratio (α_m^{E} or α_m^{C}) is a discrete variable that has at most N_{sf} candidate values. We assume the ABS ratio can be zero, but it is never to be 1. The reason has been given in Subsection II-B. The load of BS b is denoted by L_b that is an assistant variable for optimization. Once x_{ub} is given for every UE, L_b can be obtained directly.

C. OPTIMIZATION CONSTRAINTS

1) ASSOCIATION CONSTRAINTS

Each UE can only associate with a BS. The association indicator x_{ub} must satisfy this constraint:

$$\sum_{b \in \mathcal{B}} x_{ub} = 1, \quad \forall u \in \mathcal{U}. \tag{16}$$

2) LOAD STATUS CONSTRAINTS

L_b must satisfy the following constraint:

$$L_b = \sum_{u \in \mathcal{U}} x_{ub}, \quad \forall b \in \mathcal{B}. \tag{17}$$

3) DATA RATE CONSTRAINTS

When UE u is associated with BS b, let y_{ub} be the proportion of total resources UE u obtained. Taking into account constraint (16), the actual data rate of UE u is

$$r_u = \sum_{b \in \mathcal{B}} x_{ub} y_{ub} R_{ub}, \quad \forall u \in \mathcal{U}. \tag{18}$$

We assume each BS implements an independent proportional fair (PF) scheduler. Ye *et al.* [25] present that the optimal resource allocation in a PF scheduler is equal allocation. With (17), y_{ub} is equal to $1/L_b$.

Remark 3: Although we perform the resource partition in both time and frequency domains simultaneously, the conclusion in [24] still holds. Resource partition in the frequency domain is predetermined. Once ABS ratios are given, unavailable RBs for a cell is determined. These RBs can be regarded as suffering heavily fading that they cannot support any data transmission in the general scenario without such a resource partition. The resource partition has no effect on the implementation of a PF scheduler. The details of the PF scheduler we adopted is presented in Section V.

Equation (18) can be simplified to be:

$$r_u = \sum_{b \in \mathcal{B}} \frac{x_{ub} R_{ub}}{L_b}, \quad \forall u \in \mathcal{U}. \tag{19}$$

4) VALID VALUE CONSTRAINTS

x_{ub} must be binary, namely

$$x_{ub} \in \{0, 1\}, \quad \forall u \in \mathcal{U}, \ \forall b \in \mathcal{B}. \tag{20}$$

ABS ratios are discrete variables, they must follow constraints:

$$\alpha_m^{\mathrm{E}} \in \mathcal{AL}, \quad \alpha_m^{\mathrm{C}} \in \mathcal{AL}, \ \forall m \in \mathcal{M}, \tag{21}$$

where $\mathcal{AL}$ is the ABS ratio list defined in Subsection II-B. There is an implicit constraint for L_b:

$$0 \leq L_b \leq |\mathcal{U}|, \quad \forall b \in \mathcal{B}. \tag{22}$$

D. PROBLEM STATEMENT

Intuitively, if UE u is not associated with BS b, the corresponding scheduler will not assign any resource to it. Considering constraints in (16) and (20), the utility contributed by UE u is:

$$\mathrm{Util}(r_u) = \log\left(\sum_{b \in \mathcal{B}} \frac{x_{ub} R_{ub}}{L_b} \right) = \sum_{b \in \mathcal{B}} x_{ub} \log\left(\frac{R_{ub}}{L_b} \right). \tag{23}$$

The mathematical formulation of the problem for HICIC parameters optimization can be written as:

$$\begin{aligned} \mathrm{P1}: \quad & \max_{\boldsymbol{x}, \boldsymbol{L}, \boldsymbol{\alpha}^{\mathrm{E}}, \boldsymbol{\alpha}^{\mathrm{C}}} \sum_{u \in \mathcal{U}} \sum_{b \in \mathcal{B}} x_{ub} \log\left(\frac{R_{ub}}{L_b} \right) \\ & \text{s.t.} \ (16), (17), (19), (20), (21), (22), \end{aligned} \tag{24}$$

where $\boldsymbol{x}$, $\boldsymbol{L}$, $\boldsymbol{\alpha}^{\mathrm{E}}$, and $\boldsymbol{\alpha}^{\mathrm{C}}$ are vectors of the respective optimization variables. The above problem is combinatorial and the complexity of the brute force algorithm

is $\mathcal{O}\left(|\mathcal{B}|^{|\mathcal{U}|}\left(N_{sf}\right)^{2|\mathcal{M}|}\right)$. The computation is practically impossible for a typical multi-cell two-tier HetNet. In [13], a similar utility maximization problem has been formulated and the hardness of the problem has been stated. There is only one ABS ratio in each cell in [13], while problem P1 must determine two ABS ratios for the major band and the minor band of each cell. To overcome this, we design a polynomial-time semi-distributed algorithm consisting of three stages in the next section.

IV. PROPOSED ALGORITHM

The principle of our proposed scheme, named HICIC, lies in decomposing problem P1 into several single cell optimization problems, and designs a rational coordination mechanism to adjust variable parameters for the resource partition. HICIC has three stages: 1) single cell optimization, 2) cells coordination, and 3) final UE association. We will describe them in detail below. Additionally, the computational complexity is discussed at the end of this section.

A. SINGLE CELL OPTIMIZATION

In the first stage, problem P1 is decomposed into several single cell optimization problems. Two necessary assumptions are made for the problem decomposition:

- *Unified ABS ratio:* The HetNet has a unified ABS ratio. We let $\alpha_m^{\mathrm{E}} = \alpha_m^{\mathrm{C}}$, $\forall m \in \mathcal{M}$, and all MBSs are configured with the same ABS ratio.
- *Single cell association:* Each UE can only associate with BSs in the cell that it is located. It means that we deprive UEs of opportunities to be served by BSs in neighboring cells temporarily.

With these assumptions, problem P1 can be decomposed. The single cell optimization problem for cell m is written explicitly as:

$$\mathrm{P2}: \max_{\boldsymbol{x}_m, \boldsymbol{L}_m, \alpha_m^{\mathrm{E}}, \alpha_m^{\mathrm{C}}} \sum_{u\in\mathcal{U}_m}\sum_{b\in\mathcal{B}_m} x_{ub}\log\left(\frac{R_{ub}}{L_b}\right) \tag{25a}$$

$$\text{s.t.} \sum_{b\in\mathcal{B}_m} x_{ub} = 1, \quad \forall u \in \mathcal{U}_m, \tag{25b}$$

$$\sum_{u\in\mathcal{U}_m} x_{ub} = L_b, \quad \forall b \in \mathcal{B}_m, \tag{25c}$$

$$x_{ub} \in \{0,1\}, \quad \forall u \in \mathcal{U}_m, \ \forall b \in \mathcal{B}_m, \tag{25d}$$

$$\alpha_m^{\mathrm{E}} = \alpha_m^{\mathrm{C}} \in \mathcal{AL}, \tag{25e}$$

$$0 \le L_b \le |\mathcal{U}_m|, \quad \forall b \in \mathcal{B}_m, \tag{25f}$$

where $\boldsymbol{x}_m$ and $\boldsymbol{L}_m$ are vectors of corresponding variables for cell m. Problem P2 is still difficult to solve since variables x_{ub} are binary. To address this issue, all binary variables x_{ub} are relaxed to real numbers between 0 and 1. This means that a UE can be associated with multiple BSs at the same time. Beyond that, an exhaustive search through all possible ABS ratios can be performed because the size of the ABS ratio list $\mathcal{AL}$ is limited. For a given ABS ratio, P2 is simplified as a single cell UE association problem:

$$\mathrm{P3}: \max_{\boldsymbol{x}_m, \boldsymbol{L}_m} \sum_{b\in\mathcal{B}_m}\sum_{u\in\mathcal{U}_m} x_{ub}\log\left(R_{ub}\right) - \sum_{b\in\mathcal{B}_m} L_b \log L_b \tag{26a}$$

$$\text{s.t. } 0 \le x_{ub} \le 1, \quad \forall u \in \mathcal{U}_m, \ \forall b \in \mathcal{B}_m, \quad (25\text{b}), \ (25\text{c}), \ (25\text{f}). \tag{26b}$$

Problem P3 is a special case of the UE association problem in [25]. Since P3 is a convex optimization problem and the strong duality holds [25], it can be equivalently solved by its corresponding dual problem. Ye *et al.* [25] propose a primal-dual distributed algorithm to solve it. But the algorithm in [25] cannot be utilized to solve problem P3 directly. One reason is that some assistant variables for updating step size are sensitive to the ABS ratio. Another reason the more important is that we have to solve optimization problem P3 several times. Therefore, We design a centralized Load Aware UE association algorithm (LAU) mainly based on the work in [25], while some necessary modifications are conducted to enhance its robustness. Next, we will construct the dual problem for P3 and describe LAU in detail.

The object function of problem P3 is denoted by $f(\boldsymbol{x}_m, \boldsymbol{L}_m)$. By introducing a Lagrange multiplier vector $\boldsymbol{\nu}_m = \{\nu_1, \ldots, \nu_b, \ldots, \nu_{|\mathcal{B}_m|}\}$ for the coupling constraint (25c), we can form the partial Lagrangian and the dual function easily. The dual problem of P3 can be given as:

$$\mathrm{D}: \min_{\boldsymbol{\nu}_m} \quad h(\boldsymbol{\nu}_m) = h_1(\boldsymbol{\nu}_m) + h_2(\boldsymbol{\nu}_m), \tag{27}$$

where

$$h_1(\boldsymbol{\nu}_m) = \begin{cases} \max\limits_{\boldsymbol{x}_m} & \sum\limits_{b\in\mathcal{B}_m}\sum\limits_{u\in\mathcal{U}_m} x_{ub}\left(\log\left(R_{ub}\right)+\nu_b\right) \\ \text{s.t.} & \sum\limits_{b\in\mathcal{B}_m} x_{ub} = 1, \forall u \in \mathcal{U}_m, \\ & 0 \le x_{ub} \le 1, \forall u \in \mathcal{U}_m, \forall b \in \mathcal{B}_m, \end{cases} \tag{28}$$

$$h_2(\boldsymbol{\nu}_m) = \begin{cases} \max\limits_{\boldsymbol{L}_m} & \sum\limits_{b\in\mathcal{B}_m} L_b(-\log\left(L_b\right) - \nu_b) \\ \text{s.t.} & 0 < L_b \le |\mathcal{U}_m|, \forall b \in \mathcal{B}_m. \end{cases} \tag{29}$$

LAU is an iterative algorithm summarized in Algorithm 1. In the tth iteration, subproblems $h_1(\boldsymbol{\nu}_m)$ and $h_2(\boldsymbol{\nu}_m)$ are solved at first. As for the subproblem $h_1(\boldsymbol{\nu}_m)$ with given $\boldsymbol{\nu}_m$, each UE u in cell m should associate with one or more BSs from the set below:

$$\tilde{\mathcal{B}} = \left\{ b = \arg\max_{b\in\mathcal{B}_m} \left(\log\left(R_{ub}\right)+\nu_b^{(t)}\right)\right\}. \tag{30}$$

Due to the original problem P2 prefers a solution with binary components, UE u randomly selects a BS $b \in \tilde{\mathcal{B}}$ to associate. It means $x_{ub}^{(t+1)} = 1$ and $x_{ub'}^{(t+1)} = 0, \forall b' \in \mathcal{B}_m$.

Remark 4: The rounding action is conducted when the subproblem $h_1(\boldsymbol{\nu}_m)$ is solved. Therefore, the solution obtained by LAU is a suboptimal solution for the problem P3. There is an oblivious integrality gap [29].

Once $\boldsymbol{\nu}_m$ is given, the subproblem $h_2(\boldsymbol{\nu}_m)$ can be easily solved by setting the gradient of object function to be 0. It is

Algorithm 1 Load Aware UE association algorithm (LAU)

Require:
$\alpha_m^{\mathrm{E}} \in \mathcal{AL}, \alpha_m^{\mathrm{C}} \in \mathcal{AL}, \forall m \in \mathcal{M}, t = 1, \Delta = \Delta_0 = 0.5$;
$\boldsymbol{\nu}_m^{(1)}$ is initialized by arbitrary value, $\epsilon^{(1)} = \epsilon$;
Ensure:
Estimate $R_{ub}, \forall u \in \mathcal{U}_m, b \in \mathcal{B}_m$;
while $f(\boldsymbol{x}_m^{(t)}, \boldsymbol{L}_m^{(t)}) < h(\boldsymbol{\nu}_m^{(t)}) - \Delta$ **do**
  for each UE $u \in \mathcal{U}_m$ **do**
    UE u randomly selects a BS $b^* \in \tilde{\mathcal{B}}$ to associate, where $\tilde{\mathcal{B}}$ is defined in (30);
  end for
  for each BS $b \in \mathcal{B}_m$ **do**
    Update $L_b^{(t+1)}$ according to (31);
  end for
  Calculate $h_{\mathrm{best}}^{(t)}$ by (35);
  for each BS $b \in \mathcal{B}_m$ **do**
    Calculate the step size with (34);
    Update dual variables as described in (33);
  end for
  if $t > 1$ **then**
    Update $\epsilon^{(t)}$ as described in (36), Let $\epsilon^{(t+1)} = \epsilon^{(t)}$;
  end if
  $t = t + 1$;
  if t is exactly divisible by 10 **then**
    $\Delta = \Delta + \Delta_0$;
  end if
end while

of importance to note that the solution should be projected to the interval $(0, |\mathcal{U}_m|)$, i.e.,

$$L_b^{(t+1)} = \begin{cases} |\mathcal{U}_m|, & e^{(-\nu_b^{(t)}-1)} > |\mathcal{U}_m|, \\ e^{(-\nu_b^{(t)}-1)}, & \text{otherwise.} \end{cases} \tag{31}$$

The outer problem of dual variable $\boldsymbol{\nu}_m$ is solved by the subgradient method [30]. A subgradient of the dual function $h(\cdot)$ at $\boldsymbol{\nu}_m^{(t)}$ can be given easily. Its bth component is:

$$\sum_{u \in \mathcal{U}_m} x_{ub}^{(t)} - L_b^{(t)}, \quad \forall b \in \mathcal{B}_m. \tag{32}$$

Thus the dual variable for BS b is updated by:

$$\nu_b^{(t+1)} = \nu_b^{(t)} - \lambda^{(t)}\Big(\sum_{u \in \mathcal{U}_m} x_{ub}^{(t)} - L_b^{(t)}\Big), \quad \forall b \in \mathcal{B}_m, \tag{33}$$

where $\lambda^{(t)}$ is the step size dynamically updated according to the following rule:

$$\lambda^{(t)} = \gamma^{(t)} \frac{h(\boldsymbol{\nu}_m^{(t)}) - \left(h_{\mathrm{best}}^{(t)} - \epsilon^{(t)}\right)}{\|g^{(t)}\|^2}, \quad 0 < \underline{\gamma} \le \gamma^{(t)} \le \overline{\gamma} < 2, \tag{34}$$

where $\underline{\gamma}$ and $\overline{\gamma}$ are some scalars [31] and $h_{\mathrm{best}}^{(t)}$ is best value currently. At each iteration, we set

$$h_{\mathrm{best}}^{(t)} = \begin{cases} h(\boldsymbol{\nu}_m^{(1)}), & t = 1, \\ \min\{h_{\mathrm{best}}^{(t-1)}, h(\boldsymbol{\nu}_m^{(t)})\}, & t > 1. \end{cases} \tag{35}$$

And let $i_{\mathrm{best}}^{(t)} = t$ if $h(\boldsymbol{\nu}_m^{(t)}) = h_{\mathrm{best}}^{(t)}$, i.e., $\boldsymbol{\nu}_m^{(t)}$ is the best solution found so far. $\epsilon^{(t)}$ represents our desire to reach a target level that is smaller by $\epsilon^{(t)}$ over the best value achieved thus far. It is initialized by a positive constant ϵ and is updated at the end of the tth iteration ($t > 1$) according to:

$$\epsilon^{(t)} = \begin{cases} \rho\epsilon^{(t-1)}, & h(\boldsymbol{\nu}_m^{(t)}) \le (h_{\mathrm{best}}^{(t-1)} - \epsilon^{(t-1)}), \\ \max\{\theta\epsilon^{(t-1)}, \epsilon\}, & \text{otherwise,} \end{cases} \tag{36}$$

where ϵ, θ, and ρ are fixed positive constants with $\theta < 1$ and $\rho \ge 1$ [32]. To update $\epsilon^{(t)}$, we follow the rule provided in [32] but not the one utilized in [25]. This is because the subgradient method that we adopt is not a decent method. A proposition can be given to show the convergence of LAU algorithm.

Proposition 1: Assume that the step size $\lambda^{(t)}$ is determined by the dynamic rule (34) with the adjustment procedure (35) and (36). Denote the optimal value of problem D as h^*. If $h^* > -\infty$, then

$$\inf_{t \ge 1} h(\boldsymbol{\nu}_m^{(t)}) \le h^* + \epsilon. \tag{37}$$

Proof: The proof follows the same idea as that of [25, Th. 1]. Please see the references [25] and [32]. ■

Proposition 2: The termination rule is checking whether or not $f(\boldsymbol{x}_m, \boldsymbol{L}_m)$ is no less than $h(\boldsymbol{\nu}_m^{(t)}) - \Delta$, where Δ is an error tolerance initialized by a predefined value Δ_0. We will also increase Δ by Δ_0 per ten iterations. At the end of iterations, the obtained solution for UE association is pretty decent.

Proof: The proof is presented in Appendix. ■

LAU is a centralized algorithm that the MBS covering the cell is responsible to collect all necessary information and to solve the optimization problem. Designating an ABS ratio, each MBS solves problem P3 by LAU separately. An exhaustive search is conducted on all possible N_{sf} values in $\mathcal{AL}$. The ABS ratio obtaining the maximal cell-wide utility is selected as the desired ABS ratio of this MBS, denoted by α_m^{d} for cell m. If there are multiple maximizers, we will select the largest one for power saving and interference mitigation. Calculations in this stage are summarized in Algorithm 2, named Single Cell Optimization (SCO).

Algorithm 2 Single Cell Optimization (SCO)

Ensure:
for $\alpha_i \in \mathcal{AL}$ **do**
  $\alpha_m^{\mathrm{E}} = \alpha_m^{\mathrm{C}} = \alpha_i, \forall m \in \mathcal{M}$;
  for each MBS $m \in \mathcal{M}$ **do**
    Solve P3 by LAU;
    Record the optimal value of P3 as the cell-wide utility of cell m with α_i;
  end for
end for
for each MBS $m \in \mathcal{M}$ **do**
  Find the maximal cell-wide utility for cell m;
  Regard the corresponding ABS ratio (if more than one, select the largest value) as its desired ABS ratio α_m^{d} ;
end for

B. CELLS COORDINATION

In the second stage, coordinations among cells are necessary. MBS m must send its desired ABS ratio to MBSs in its coordination neighbor list $\mathcal{CL}_m$. Accordingly, it also receives related demand information from MBSs in its request neighbor list $\mathcal{RL}_m$.

We give up the *unified ABS ratio* assumption utilized in the first stage. More reasonable ABS ratios are calculated for the major band and the minor band of each MBS. Since the minor band has relatively lower transmission power, its division in the time-domain will have little effects on neighboring cells. We regard the desired ABS ratio of cell m obtained in the first stage, α_m^{d}, as the ABS ratio of its minor band, namely $\alpha_m^{\mathrm{C}} = \alpha_m^{\mathrm{d}}$. Before calculating the ABS ratio of the major band, we introduce a novel concept named coordination willingness. For MBS m, its coordination willingness is defined by:

$$\omega_m = \begin{cases} 0, & \mathcal{RL}_m = \emptyset, \\ \dfrac{\left(\alpha_m^{\mathrm{d}} + \left(1 - \frac{1}{|\mathcal{RL}_m|}\right)\right)}{2}, & \text{otherwise}, \end{cases} \tag{38}$$

where $|\cdot|$ returns the cardinality of the corresponding set. It is evident that two equally important factors affect the coordination willingness of an MBS.

- The first factor is its own desired ABS ratio. Its coordination willingness is increasing with the increase in its demand.
- The second factor is the size of its request neighbor list. For any MBS, the more neighboring MBSs make requests to it, the more willingness to coordinate it has.

Since $0 \le \alpha_m^{\mathrm{d}} < 1$ and $|\mathcal{RL}_m| \ge 1$, the coordination willingness of MBS m satisfies $0 \le \omega_m < 1$. Fig. 3 presents some coordination willingness for illustration. The ABS ratio of the major band of MBS m is a weighted summation of its own demand α_m^{d} and the average demand of MBSs in its request neighbor list. It can be estimated by the following equation:

$$\tilde{\alpha}_m^{\mathrm{E}} = (1 - \omega_m)\,\alpha_m^{\mathrm{d}} + \omega_m \frac{\sum_{m' \in \mathcal{RL}_m} \alpha_{m'}^{\mathrm{d}}}{|\mathcal{RL}_m|}. \tag{39}$$

If MBS m has a strong willingness to coordinate, it puts a greater emphasis on the requirements of neighbors; otherwise, it will be selfish. As an ABS ratio is a discrete value, it must be rounded by the rounding function below:

$$\mathrm{Rnd}_{N_{sf}}(\alpha) = \begin{cases} \dfrac{\lfloor \alpha N_{sf} \rfloor}{N_{sf}}, & \alpha \ge 0.5, \\ \dfrac{\lceil \alpha N_{sf} \rceil}{N_{sf}}, & \alpha < 0.5. \end{cases} \tag{40}$$

Therefore, the ABS ratio of the major band of cell m is

$$\alpha_m^{\mathrm{E}} = \mathrm{Rnd}_{N_{sf}}\left(\tilde{\alpha}_m^{\mathrm{E}}\right). \tag{41}$$

After α_m^{E} is obtained, MBS m must broadcast both α_m^{E} and α_m^{C} to all other BSs in the HetNet. By doing so, the main purpose is for calculating the collision probability and estimating the interference. Thus far, we have completed all that for the resource partition.

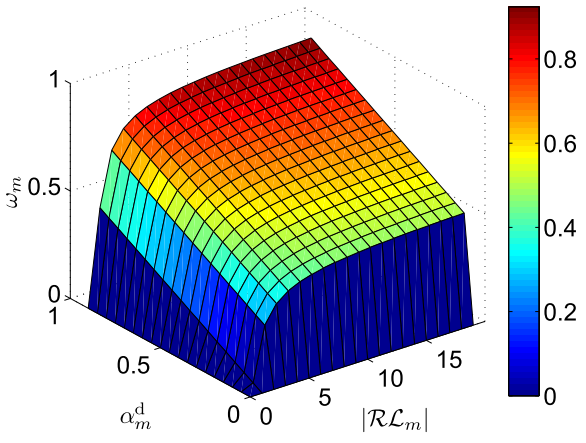

FIGURE 3. Illustration of some coordination willingness values.

C. FINAL UE ASSOCIATION

In the third stage, each MBS should implement LAU algorithm again to determine the UE association relationships, then resource partition patterns and user association indicators are all available. Afterwards, we give up the *single cell association* assumption in the first stage and design a method to realize load balance among cells. It keeps monitoring the status of the HetNet and triggers a handoff among cells whenever it is necessary.

Some UEs near boundaries of two cells may contribute more to the summation utility if they are associated with neighboring MBSs. We have assumed in Subsection III-C that each BS implements a proportional fair scheduler independently. The multi-user diversity gain (scheduling gain) of a practical scheduler can be taken into consideration for estimating data rates of UEs. The actual data rate of UE u who is associated with BS b can be rewritten as:

$$r_u = \frac{G(L_b)\,R_{ub}}{L_b}, \tag{42}$$

where $G(L_b)$ is the average scheduling gain of BS b. Son *et al.* [33] propose an estimation method to obtain the scheduling gain by doing calculations in a predefined time window. A UE near cell boundaries can change its association from BS b to BS b' if the following condition is satisfied:

$$\frac{G(L_b)\,R_{ub}}{L_b} + \phi \le \frac{G(L_{b'})\,R_{ub}}{L_{b'} + 1}, \tag{43}$$

where b and b' belong to different cells, and ϕ is a handover threshold to avoid the ping-pong effect. Note that we utilize $G(L_{b'})$ as an approximation of $G(L_{b'} + 1)$ because the latter one is not available actually. This approximation works when the number of UEs associated with BS

b' is large enough. Hence, only MBS to MBS handover is permitted in general. Each MBS accepts only one additional UE unless its scheduling gain is updated.

D. COMPLEXITY ANALYSIS

Both the time complexity and the convergence property of HICIC are analyzed in this subsection. For cell m, LAU is implemented N_{sf} times in the first stage. In the second stage, ABS ratios are calculated directly after the information exchange among cells completed. There are two parts in the third stage: in the former part, each cell implements LAU one more time; in the latter part, each cell updates its scheduling gain and determines whether or not a handoff among cells should be triggered according to a simple comparing criteria. Hence there is no other iterative calculations in HICIC except LAU. The convergence speed of LAU is determinant of the convergence property of HICIC. The computational complexity of LAU is mainly determined by three factors:

- the cost of estimating R_{ub};
- the cost of operations in an outer iteration;
- the number of iterations until termination, T.

As shown in Subsection IV-A, subproblems for UEs and BSs have been decoupled so that they can be solved separately. Dual variables and other assistant variables can also be updated directly. The time complexity to estimate R_{ub} for all UEs in cell m is $\mathcal{O}(|\mathcal{B}_m||\mathcal{U}_m|)$. The time complexity to determine association relationships for UEs in cell m is $\mathcal{O}(|\mathcal{U}_m|)$. That of updating the desired load for BSs in cell m is $\mathcal{O}(|\mathcal{B}_m|)$. The time complexity to update dual variables and to prepare assistant variables for the next iteration is also $\mathcal{O}(|\mathcal{B}_m|)$. Other if statements have a time complexity of $\mathcal{O}(1)$. Although the subgradient method is not a decent method, it converges fast in general. Values of object functions in the iteration process of LAU will be illustrated in the next section to verify that T is a small number (less than 20) in most cases. However, as the integrality gap cannot be obtained in advance, very few cells suffer from a relatively larger T no more than 60. All in all, the convergence of HICIC is guaranteed. Since $|\mathcal{U}_m| > |\mathcal{B}_m|$ holds generally, the time complexity of LAU is $\mathcal{O}(|\mathcal{B}_m||\mathcal{U}_m| + T|\mathcal{U}_m| + T|\mathcal{B}_m|) = \mathcal{O}(|\mathcal{U}_m|(|\mathcal{B}_m| + T))$. As each cell runs LAU independently, so the time complexity of HICIC is $\mathcal{O}(N_{sf}|\mathcal{U}_m|(|\mathcal{B}_m| + T))$.

V. NUMERICAL RESULTS AND DISCUSSIONS

A. SIMULATION SCENARIO

The performance of HICIC is evaluated through a dynamic LTE-FDD system level simulator utilizing MATLAB. Necessary simulation parameters listed in Table 2 are per the 3GPP simulation guidelines in [1]. Two different non-uniform topologies are simulated.

1) Simple topology: There are 2 tri-sectorized sites with 6 MBSs. Cells 3 and 6 each have 4 PBSs. The ABS ratio is restricted to be a binary value, 0 or 0.9, under this topology.
2) Complex topology: There are 19 tri-sectorized sites with a total of 57 MBSs in a wrap-around structure. Cells in $\{3(n-1)+1, n=1, 2, \ldots, 19\}$ are overlaid with PBSs, and each cell has 4 PBSs uniformly distributed. ABS ratios are selected from the ABS ratio list in Table 2.

TABLE 2. Simulation parameters.

Parameter	Value
Number of MBSs	2 tri-sectorized sites with 6 MBSs; 19 tri-sectorized sites, wrap around with a total of 57 MBSs
Number of PBSs per cell	0 or 4
Number of UEs per cell	30 or 60
MBSs inter-site distance	500 m
Min PBS-MBS distance	75 m
Min PBS-PBS distance	40 m
Min UE-MBS distance	35 m
Min UE-PBS distance	10 m
Carrier frequency	2 GHz
System bandwidth	10 MHz
Number of subchannels	48 for PDSCH, 2 for PDCCH
ABS period	10 subframes
ABS ratio list	0,0.1,0.2,0.3,0.4,0.5,0.6,0.7,0.8,0.9
MBS/PBS Tx power	46 dBm/30 dBm
MBS antenna gain	$A(\theta) = -\min\left[12\left(\frac{\theta}{\theta_{3\text{dB}}}\right)^2, A_m\right] + B$ $A_m = 20$ dB, $B = 15$ dBi, $\theta_{3\text{dB}} = 65°$, $-180° \le \theta \le 180°$
MBS pathloss model	$L = 128.1 + 37.6\lg(d)$, d in km
PBS antenna gain	omnidirectional, 5 dBi gain
PBS pathloss model	$L = 140.7 + 36.7\lg(d)$, d in km
Shadowing standard deviation	8 dB
Shadowing correlation distance	50 m
Inter-MBS correlation	0.5
Intra-MBS correlation	1
UE noise figure	9 dB
Thermal noise density	-174 dBm/Hz
Traffic type	full buffer
UE mobility	3 km/h
BS scheduler	proportional fair
Target BER	10^{-6}
RSRP threshold P_{th}	-70 dBm

As described in [1], the UE density is defined as the number of UEs in the geographic area of a cell. The PBS density should be proportional to the UE density in each cell. We assume that 30 UEs are distributed uniformly in a cell without PBSs. As for a cell overlaid with PBSs, there are 60 UEs in total. Within 45 meters of each PBS, 10 UEs are distributed uniformly. Other 20 UEs are distributed uniformly in the whole cell.

B. COMPARATIVE SCHEMES

HICIC is compared with other seven schemes and all comparative schemes are listed in Table 3. We will explain the components simply below:

- **SFR**: SFR follows descriptions in Subsection II-B with $\beta^{\text{NC}} = \frac{1}{16}$, $\beta^{\text{AE}} = \frac{1}{4}$, and $\beta^{\text{AC}} = 0$.
- **Reuse 1**: Reuse the total spectrum in all cells without any power restriction.
- **Unified**: A unified ABS ratio is adopted across the whole HetNet. All possible values in the ABS ratio list of Table 2 will be simulated.

TABLE 3. Comparative schemes.

Scheme	Reuse	ABS ratio	Dummy BS	Association
HICIC	SFR	Hybrid	H&L	LAU
USHL	SFR	Unified	H&L	LAU
HSAN	SFR	Hybrid	A&N	LAU
USAN	SFR	Unified	A&N	LAU
HRAN	Reuse 1	Hybrid	A&N	LAU
URAN	Reuse 1	Unified	A&N	LAU
FIXED1	Reuse 1	0.1	None	5dB bias
FIXED2	Reuse 1	0.4	None	12dB bias

- **Hybrid**: ABS ratios are determined by the method in Subsection IV-B.
- **H&L**: An MBS is regarded as two dummy BSs, HPD and LPD described in Subsection II-B.
- **A&N**: An MBS is visualized as two dummy BSs: one works in ABS subframes and the other one works in non-ABS subframes. This idea comes from [22].
- **LAU**: UE association relationships are determined by LAU proposed in Subsection IV-A.
- **FIXED1 and FIXED2**: The unified ABS ratio of FIXED1 is 0.1. UEs are associated with BSs following max-RSRP rule with 5dB bias for PBSs. The ABS ratio of FIXED2 is 0.4 and the bias value is 12 dB.

All comparative schemes only provide resource partition patterns and UE association relationships. With these information, each BS will implement an independent proportional fair scheduler to serve UEs. We run the simulation for 100 ABS periods.

The implementation of a PF scheduler is described in detail below. We allocate all available RBs at the time slot t to the selected UE. Another alternative choice is allocating RBs one by one. Each BS would like to select the optimal UE to serve at the time slot t according to the following rule:

$$\hat{u}_b(t) = \arg\max_{u \in \mathcal{U}_b} \frac{r_u(t)}{\bar{r}_u(t-1)}, \tag{44}$$

where $r_u(t)$ is the instant data rate of UE u at the slot t, and $\bar{r}_u(t-1)$ is its k-point moving average throughput at the previous slot. $\bar{r}_u(t)$ is updated by:

$$\bar{r}_u(t) = \left(1 - \frac{1}{k}\right)\bar{r}_u(t-1) + \frac{1}{k} I_{ub}(t) r_u(t), \tag{45}$$

where $I_{ub}(t)$ is an indicator function of the event that UE u is selected at the slot t. It is defined by:

$$I_{ub}(t) = \begin{cases} 1, & u = \hat{u}_b(t), \\ 0, & \text{otherwise}. \end{cases} \tag{46}$$

C. NUMERICAL RESULTS

The simple topology is shown in Fig. 4(a). System utilities of schemes under this topology are compared in Fig. 5. The unit of UE rates in calculations of the system utility is bits/s. Since the ABS ratio can be only 0 or 0.9, FIXED1 and FIXED2 are not considered under this topology. OPT is the optimal ABS configuration for our proposed BS structure. It is obtained

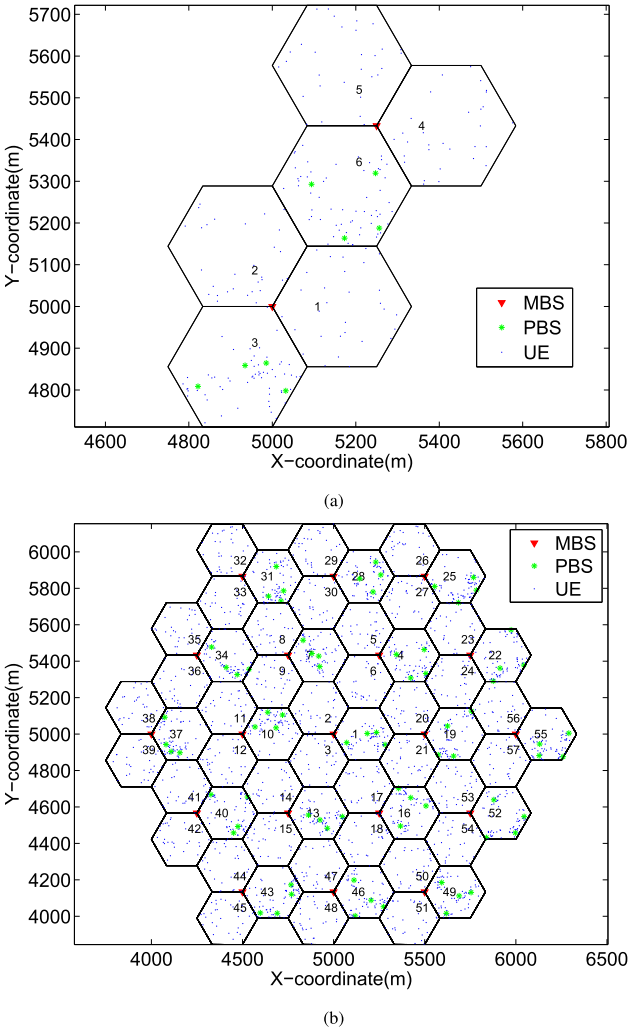

FIGURE 4. Network topologies.

by conducting a brute force search on all $2^{12} = 4096$ ABS configurations. Given an ABS configuration, the binary variable x_{ub} is relaxed and problem P1 is transformed into a convex problem that can be solved easily. Therefore the utility provided by OPT is a loose upper bound for HICIC. As depicted in Fig. 5, although HICIC do well under this topology, there is an obvious gap between HICIC and OPT. The reason behind this is that these two schemes have the same ABS ratio vector for the minor band, namely $\boldsymbol{\alpha}^{\mathrm{C}} = \{0, 0, 0.9, 0, 0, 0.9\}$, but different ABS ratio vectors for the major band. OPT configures $\boldsymbol{\alpha}^{\mathrm{E}} = \{0.9, 0.9, 0.9, 0, 0, 0.9\}$, while HICIC has $\boldsymbol{\alpha}^{\mathrm{E}} = \{0, 0, 0.9, 0, 0, 0.9\}$. Obviously, if cell 1 and cell 2 can take part in the collaboration, the system utility can be further improved. However, our proposed coordination mechanism is insensitive when the size of the request neighbor list is small. It is a shortcoming of our proposed coordination mechanism, while this disadvantage can be weakened in the complex topology because the possibility of a cell having a relatively larger request neighbor list increases. For schemes with unified ABS configurations,

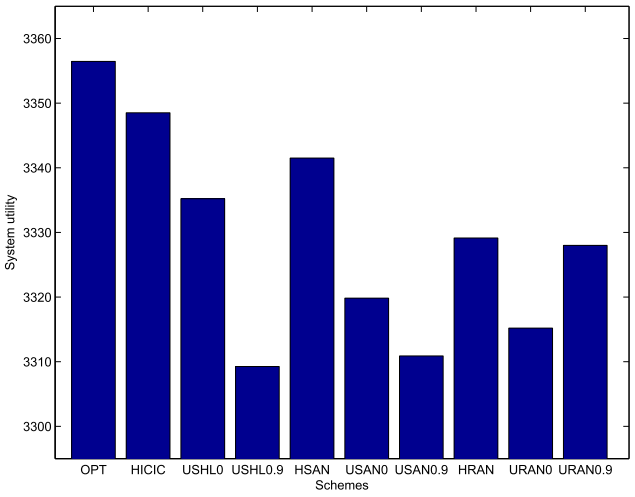

FIGURE 5. Comparison of the system utility under the simple topology.

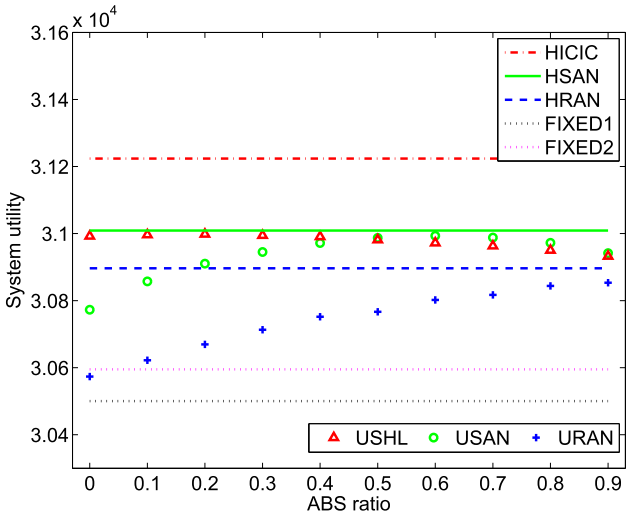

FIGURE 6. Comparison of the system utility under the complex topology.

both USHL and USAN prefer null ABS ratio to obtain the higher system utility, while URAN desires the ABS ratio to be 0.9. It indicates that cells must be selfless to coordinate for mitigating interference as SFR is absent in URAN. Apart from this, an important conclusion can be claimed that any scheme with a hybrid ABS configuration is superior than the corresponding scheme with a unified ABS ratio under this topology, such as HICIC is better than USHL. This is explained by the fact that the demand of each cell has been considered for determining a reasonable hybrid ABS configuration.

The achievable system utility is heavily dependent on the network topology. Therefore we also do simulations under the complex topology illustrated in Fig. 4(b). In contrast to the simple topology, the HetNet becomes more complicated and the coupling relationships are tightened since more PBSs are deployed. Part of coordination results of HICIC is listed in Table 4. Results of HSAN and HRAN are similar to that of HICIC. With the predefined RSRP threshold $P_{th} = -70$dBm, only some of the first tier neighboring cells are incorporated into the coordination neighbor list. A cell with PBSs configures both the major band and the minor band with the maximal ABS ratio. However, a cell without PBSs desires a small ABS ratio, but it will make reasonable sacrifices to assist other cells who need large ABS ratios.

TABLE 4. Part of coordination results.

Cell ID	$\mathcal{CL}$	$\mathcal{RL}$	α^{C}	α^{E}
1	2,3,21	$\emptyset$	0.9	0.9
2	$\emptyset$	1,7,10	0	0.3
3	$\emptyset$	1	0	0
4	5,6,20,23,24	$\emptyset$	0.9	0.9
5	$\emptyset$	4,28	0	0.2
6	$\emptyset$	4	0	0
7	2,8,9,30	$\emptyset$	0.9	0.9
8	$\emptyset$	7,31	0	0.2
9	$\emptyset$	7,10,34	0	0.3
10	$\emptyset$	2,9,11,12	0.9	0.9

In Fig. 6, system utility values of all comparative schemes in the last subsection are compared under the complex topology. We omit the OPT solution due to its large time complexity for all 10^{114} ABS configurations. FIXED1 and FIXED2 are the two worst schemes since their system parameters are fixed and not suitable to the considered topology. No matter unified or hybrid ABS configurations, a scheme with SFR always have better performance than its counterpart with reuse 1. This proves the necessity of SFR to mitigate ICI in such a two-tier HetNet with non-uniform topology. For the three schemes with unified ABS ratios and dummy BSs, results of the zero ABS ratio are important. In this case, there is no any ABS subframes that eICIC does not work. USAN is better than URAN since power restrictions are applied on different subbands according to SFR. However, each MBS has no dummy BSs with URAN or USAN actually. Our proposed dummy BS structure is working in USHL and it makes good use of SFR bringing further performance improvement. For schemes with hybrid ABS configurations, HICIC keeps being the strongest performer in system utility that it maintains its absolute advantage over others. However, HSAN has no definitely superiority than schemes with unified ABS configurations. It is caught up by USHL with ABS ratio 0.2 and by USAN with ABS ratio 0.6. This has reaffirmed the necessity of our proposed dummy BS structure.

Note that UEs with high SINRs are the primary sources of the system utility, so differences in system utilities among different schemes are small. However, the improvement coming from a hybrid ABS configuration is necessary for UEs with geographical disadvantages. These UEs are major concerns of interference coordination schemes. They have relatively low data rates for various reasons. To understand the effect on these UEs, we present the cumulative distribution function (CDF) of UEs data rate in Fig. 7. Only the three schemes with hybrid ABS configurations and the

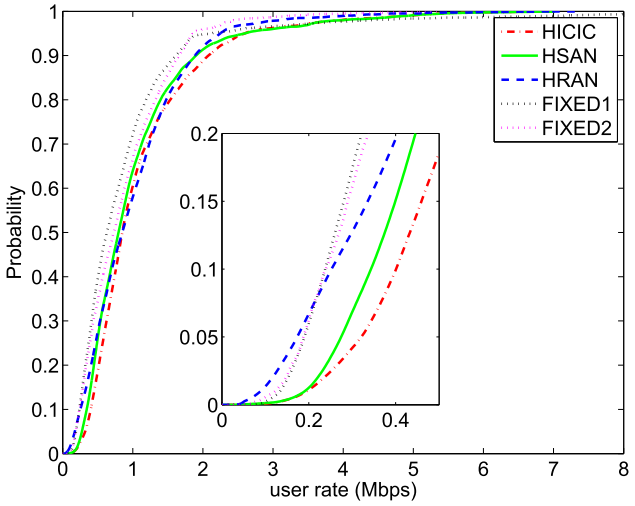

FIGURE 7. CDF of UEs data rate under the complex topology.

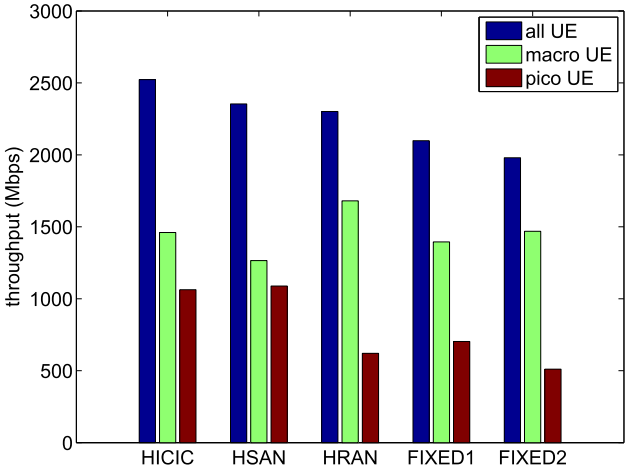

FIGURE 9. Comparison of sum throughput of UEs under the complex topology.

two schemes with fixed ABS ratios are considered. The 5th percentile UE data rate of HICIC is 0.321Mbps. It has an increase of 85.5% compared to that of HRAN, 0.173Mbps, and an increase of 17.2% compared to HSAN, 0.274Mbps. For the 10th percentile UE data rate, the corresponding gains are 57.9% and 16.6%, respectively. This verifies that both SFR and the novel dummy BS structure make contributions to the performance improvement for UEs with geographical disadvantages.

As other important performance measures, Fig. 8 and 9 present the Jain's fairness index (JFI) and throughput of UEs, respectively. The JFI of all UEs is defined as [34]:

$$JFI = \left(\sum_{u\in\mathcal{U}} r_u\right)^2 \Big/ \left(|\mathcal{U}| \sum_{u\in\mathcal{U}} r_u^2\right). \tag{47}$$

If all UEs get the same data rate, then JFI is 1. As the disparity increases, JFI decreases to 0. It is easy to write JFI expressions

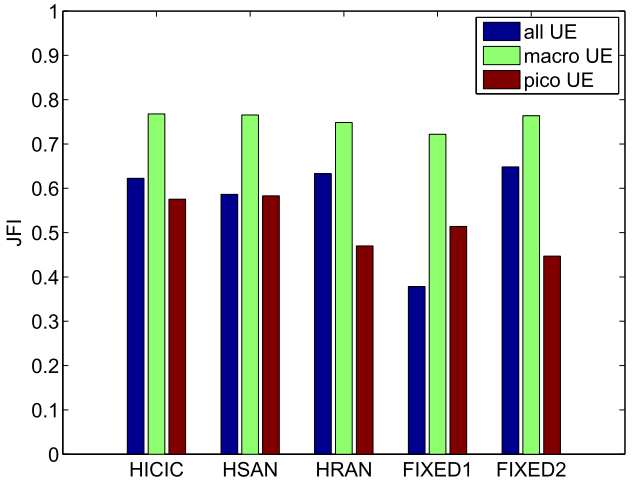

FIGURE 8. Comparison of JFI of UEs under the complex topology.

for macro UEs or pico UEs referring to (47). Surprisingly, FIXED2 has the largest JFI of all UEs, while its throughput of all UEs is the smallest in Fig. 9. It indicates that data rates of most UEs in FIXED2 are relatively low. For each scheme, the JFI of macro UEs is much greater than that of pico UEs. This occurs because the interference environment facing by pico UEs is more complicated. With the utilization of SFR and dummy BS structures, we can see that the sum throughput of UEs of HICIC has an increase of 7.2% compared to that of HRAN in Fig. 9, while that of macro UEs suffers a decrease of 13.1%. It means that the HetNet has taken full advantage of PBSs. From the system perspective, HICIC and HSAN improve the sum throughput of all UEs. At the same time, HICIC and HSAN have losses compared to HRAN in JFI. This is in consistent with the fact that there is a tradeoff of these two metrics in general. We can claim HICIC is better than HSAN as there are improvements in both JFI and throughput of all UEs. The throughput of pico UEs of HICIC is almost equal to that of HSAN. Obviously, the gain of sum throughput of all UEs is derived from macro UEs. The restriction on the transmission power of some RBs at MBSs is unfavorable to macro UEs, but HICIC compensate them.

To further validate the advantage of HICIC, an enlarged view of UE association relationships is demonstrated in Fig. 10. As depicted in Fig. 10(a) and (b), UEs are offloaded to PBSs effectively with HICIC and HSAN. This proves that the gain of system utility of HICIC compared to HSAN stems from the novel dummy BS structure and that macro UEs is the main interest group. However, the performance of HRAN is less impressive. The reason behind this is that the absence of SFR limits its ability to mitigate interference from adjacent MBSs. As depicted in Fig. 10(e), the bias of FIXED1, 5dB, is too small to offload UEs from MBSs to PBSs. With 12dB bias, PBSs become more attractive in Fig. 10(f). Nevertheless, FIXED2 does not consider the distribution of UEs resulting

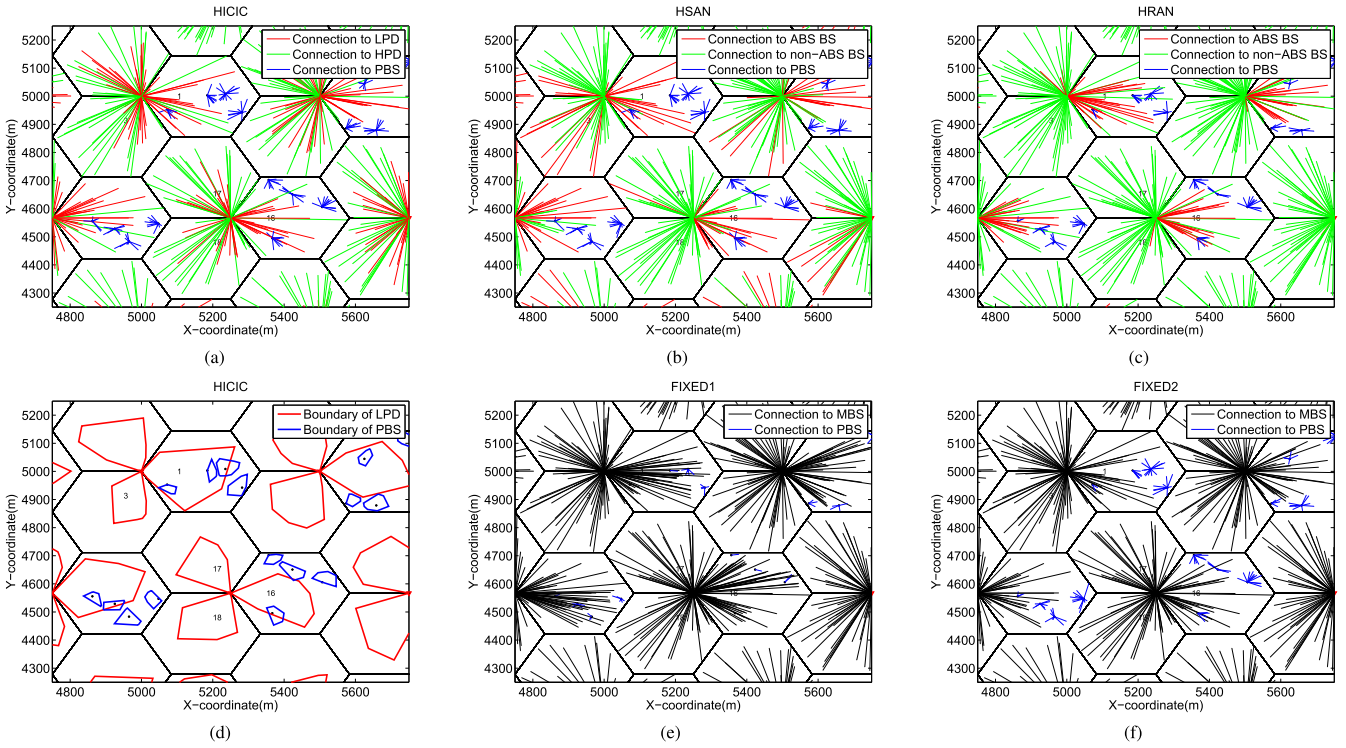

FIGURE 10. Illustration of UE association relationships. (a) UE association with HICIC. (b) UE association with HSAN. (c) UE association with HRAN. (d) Cell structure with HICIC. (e) UE association with FIXED1. (f) UE association with FIXED2.

most PBSs are still underloaded. Although there is no UEs classification, macro UEs are separated into two groups in Fig. 10(a), (b), and (c) because dummy BS structures are adopted. The boundary of LPD is estimated in Fig. 10(d) by the convex hull of locations of all UEs associated with it, so is a PBS. Loads of two dummy BSs, namely LPD and HPD, belong to the same MBS are balanced and the resulting cell structure is similar to the standard SFR [3]. An LPD in a cell with PBSs has a little larger coverage region than the one in a cell without any PBSs. This is in accordance with the coordination results in Table 4 that cells with PBSs have much greater ABS ratios. Therefore these LPDs have more resources to attract UEs, but some UEs have been offloaded to PBSs. That's why the difference is limited. Nevertheless, in a cell without PBSs, there are few or no UEs associating with ABS BSs. It is difficult to draw boundaries of ABS BSs for all cells in HSAN and HRAN. This validates our declaration in Section I that HICIC can inherit the conciseness and efficiency of SFR.

Additionally, we analyze the effect of relative power reduction ratios, namely β^{NC}, β^{AE}, and β^{AC}, on the system utility of HICIC. Eight different combinations of relative power reduction ratios are listed in Table 5 and system utilities are compared in Fig. 11. With the first four combinations where $\beta^{\mathrm{NC}} = \beta^{\mathrm{AE}} = \beta^{\mathrm{AC}}$, the system utility is inversely proportional to the transmission power. C4 is also the most satisfactory one among all combinations in Table 5. The reason behind this is that coupling relationships of cells are softened

TABLE 5. Relative power reduction ratios.

Name	β^{NC}	β^{AE}	β^{AC}
C1	1/2	1/2	1/2
C2	1/4	1/4	1/4
C3	1/8	1/8	1/8
C4	1/16	1/16	1/16
C5	1/16	1/4	0
C6	1/4	0	1/4
C7	1/4	1/4	1/16
C8	1/4	1/4	0

when MBSs are configured with a relatively lower transmission power. C5 is the configuration adopted in simulations above, while its performance belongs to the middle ones. Notwithstanding, C5 is a good choice to guarantee the data rate of macro UEs. To verify this, we show the CDF of data rate of UEs with different combinations in Fig. 12. The bottom portion of Fig. 12 shows that the performance of C5 is the best in both the 5th percentile and the 10th percentile of data rate of UEs. However, β^{AC} is zero in C5 that it results in losses of available resources, especially for an MBS with a large ABS ratio for its minor band. How to configure more reasonable power reduction ratios for different purposes is one of our future work.

As the performance of LAU algorithm is crucial to the whole scheme, its iteration processes in some cells are illustrated in Fig. 13. The dual object is $h(\boldsymbol{v}_m^{(t)})$ calculated by equation (27) and the primal object is the value of $f(\boldsymbol{x}_m, \boldsymbol{L}_m)$

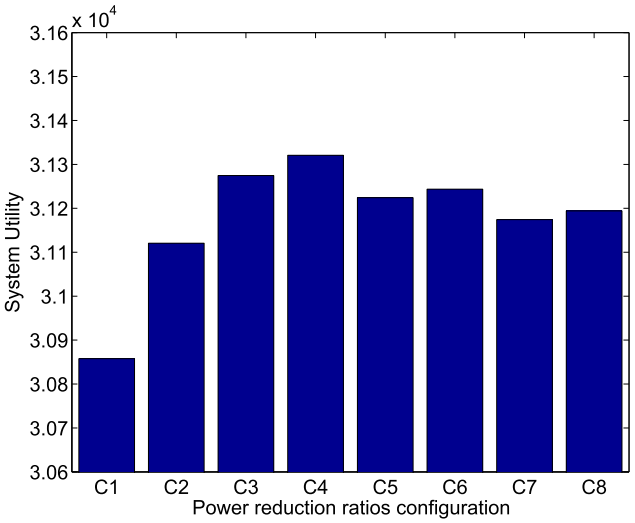

FIGURE 11. Comparison of system utility with different relative power reduction ratios under the complex topology.

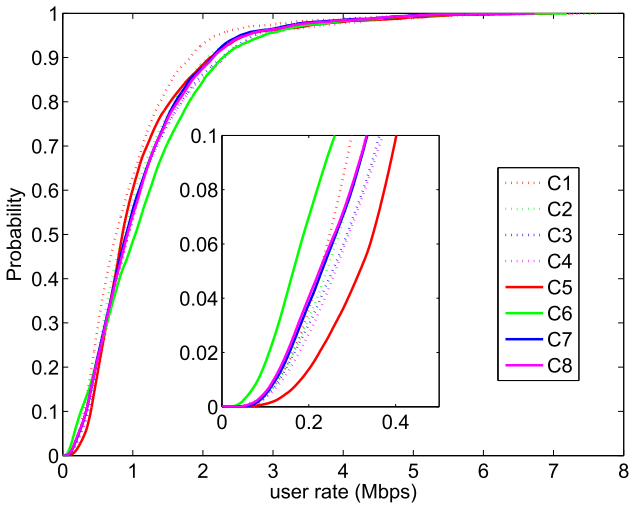

FIGURE 12. CDF of UEs data rate with different relative power reduction ratios under the complex topology.

in equation (25a). We let $\epsilon = 1$, $\theta = 0.1$, $\rho = 1.8$. It can be seen from Fig. 13 that no matter whether a cell is overlapped by PBSs or not, LAU algorithm has rapid rate to convergence. Obviously, values of the dual object confirms the fact that the subgradient method is not a decent method. Traditionally, such an iterative algorithm terminates when the difference between the current dual object value and that of last iteration is small enough. In Fig. 13(a), it may stop at the 14th iteration with the traditional rule of termination, while the performance of the corresponding primal object is poor. Similarly, the result of the 12th or 16th iteration is also unsatisfactory in Fig. 13(b). Consequently, the termination rule we declared in Proposition 2 is reasonable and effective. In addition, the result of the 4th iteration in Fig. 13(a) and that of the 6th iteration in Fig. 13(b) are good enough. However,

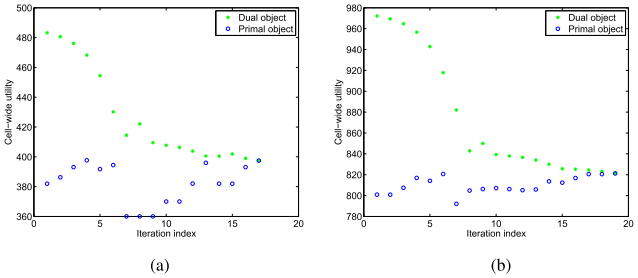

FIGURE 13. Converge evaluation for the LAU algorithm. (a) A cell without PBSs. (b) A cell with PBSs.

we cannot design a rule to terminate the algorithm at these instants. This is also left as our future work.

VI. CONCLUSIONS

In this paper, a novel interference coordination framework, named HICIC, is proposed for pursuing the maximum logarithm utility in a two-tier HetNet with a non-uniform topology. HICIC incorporates three stages to determine ABS ratios and UE association relationships. In the first stage, an MBS considers the requirement of every PBS located in its coverage area to determine the desired ABS ratio maximizing the cell-wide utility. In the second stage, an MBS plays as a representative of all BSs in its cell. It negotiates with some neighboring MBSs to determine ABS ratios by utilizing the coordination willingness. In the third stage, UE association relationships can be calculated with the proposed LAU algorithm and an assistant inter-cell load balance method. Accompany with the novel dummy BS structure, HICIC inherits the conciseness and efficiency of the standard SFR. Numerical results demonstrate that HICIC can make a HetNet with a non-uniform topology more efficient and keep fairness among UEs. Our work verifies that ICIC and eICIC/FeICIC are not either-or propositions. Future work could include efficient algorithms to estimate the desired ABS ratio of an MBS, detailed definitions of coordination willingness with consideration of more factors, and applications in ultra dense networks (UDNs).

APPENDIX

PROOF OF PROPOSITION 2

We present the proof by decomposing the difference between $f(\boldsymbol{x}_m, \boldsymbol{L}_m)$ and $h(\boldsymbol{\nu}_m^{(t)})$ into three parts.

Firstly, the rounding action is taken place in solving the subproblem $h_1(\boldsymbol{\nu}_m)$ of D. It is obvious that the object value of $h_1(\boldsymbol{\nu}_m)$ with a binary solution is no worst than that of $h_1(\boldsymbol{\nu}_m)$ with a fractional solution. We can rest assured that there is no loss of system utility in this process. This means the difference between f and f_{binary} is limited.

Secondly, relationships of object values are illustrated in Fig. 14 referring to [35]. We prove P3 is a convex optimization problem in Proposition 1 and find out that the strong duality holds. Therefore the duality gap should be zero with fractional optimal solutions, namely $f^* = h^*$. Although

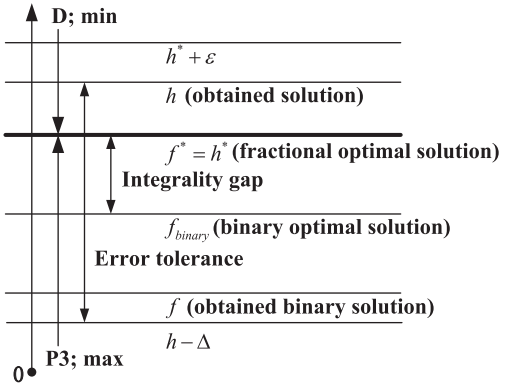

FIGURE 14. Relationships of object values.

the subgradient method is not a decent method, it converges fast in general. According to Lemma 1, the object value of problem D with the obtained solution will be no more than $h^* + \epsilon$. This means the difference between h^* and h is under control.

And lastly, as shown in Fig. 14, the error tolerance is more tolerant than the integrality gap, the difference between f^* and f_{binary}. However, the integrality gap can never be obtained in advance, so we increase the error tolerance per ten iterations with a predefined step size Δ_0.

Overall, a suboptimal solution for the dual problem D does not guarantee a satisfactory solution for the primal problem P3. We must select a relatively better solution for P3 after the process of solving D is converged. So we adopt the termination rule that it inspects whether or not $f(\boldsymbol{x}_m, \boldsymbol{L}_m)$ is no less than $h(\boldsymbol{v}_m^{(t)}) - \Delta$, where Δ is an dynamic update error tolerance. We can be confident that the obtained solution for UE association is pretty decent at the end of iterations.

REFERENCES

[1] *Evolved Universal Terrestrial Radio Access (E-UTRA); Further Advancements for E-UTRA Physical Layer Aspects (Release 9)*, document TS 36.814, 3GPP, Mar. 2010.
[2] *Evolved Universal Terrestrial Radio Access (E-UTRA) and Evolved Universal Terrestrial Radio Access Network (E-UTRAN); Overall Description; Stage 2 (Release 8)*, document TS 36.300, 3GPP, Dec. 2008.
[3] *Soft Frequency Reuse Scheme for UTRAN LTE*, document R1-050507, Huawei 3GPP, May 2005.
[4] *Inter-Cell Interference Handling for E-UTRA*, document R1-050764, Ericsson, 3GPP, Sep. 2005.
[5] *Interference Mitigation—Considerations and Results on Frequency Reuse*, document R1-050738, Siemens, 3GPP, Sep. 2005.
[6] M. Yassin *et al.*, "Survey of ICIC techniques in LTE networks under various mobile environment parameters," *Wireless Netw.*, vol. 23, no. 2, pp. 403–418, Feb. 2017.
[7] *Requirements for Further Advancements for E-UTRA (LTE-Advanced) (Release 11)*, document TS 36.913, 3GPP, Sep. 2012.
[8] *Evolved Universal Terrestrial Radio Access (E-UTRA); Mobility Enhancements in Heterogeneous Networks (Release 11)*, document TS 36.839, 3GPP, Sep. 2012.
[9] *Scenarios for eICIC Evaluations*, document R1-112543, Qualcomm, 3GPP, Aug. 2011.
[10] Y. Wang and K. I. Pedersen, "Performance analysis of enhanced inter-cell interference coordination in LTE-advanced heterogeneous networks," in *Proc. 75th Veh. Technol. Conf. (VTC Spring)*, Yokohama, Japan, May 2012, pp. 1–5.
[11] J. Pang, J. Wang, D. Wang, G. Shen, Q. Jiang, and J. Liu, "Optimized time-domain resource partitioning for enhanced inter-cell interference coordination in heterogeneous networks," in *Proc. IEEE Wireless Commun. Netw. Conf. (WCNC)*, Shanghai, China, Apr. 2012, pp. 1613–1617.
[12] A. Tall, Z. Altman, and E. Altman, "Self organizing strategies for enhanced ICIC (eICIC)," in *Proc. 12th Int. Symp. Modeling Optim. Mobile, Ad Hoc, Wireless Netw. (WiOpt)*, Hammamet, Tunisia, May 2014, pp. 318–325.
[13] S. Deb, P. Monogioudis, J. Miernik, and J. P. Seymour, "Algorithms for enhanced inter-cell interference coordination (eICIC) in LTE HetNets," *IEEE/ACM Trans. Netw.*, vol. 22, no. 1, pp. 137–150, Feb. 2014.
[14] H. Zhou, Y. Ji, X. Wang, and B. Zhao, "ADMM based algorithm for eICIC configuration in heterogeneous cellular networks," in *Proc. IEEE Conf. Comput. Commun. (INFOCOM)*, Hong Kong, Apr./May 2015, pp. 343–351.
[15] T.-Q. Zhou, Y.-M. Huang, and L.-X. Yang, "Joint user association and resource partitioning with QoS support for heterogeneous cellular networks," *Wireless Pers. Commun.*, vol. 83, no. 1, pp. 383–397, Jul. 2015.
[16] A. Liu, V. K. N. Lau, L. Ruan, J. Chen, and D. Xiao, "Hierarchical radio resource optimization for heterogeneous networks with enhanced inter-cell interference coordination (eICIC)," *IEEE Trans. Signal Process.*, vol. 62, no. 7, pp. 1684–1693, Apr. 2014.
[17] W.-C. Pao, J.-W. Lin, Y.-F. Chen, and C.-L. Wang, "Joint ABS and user grouping allocation for HetNet with picocell deployment in downlink," *EURASIP J. Wireless Commun. Netw.*, vol. 2017, no. 1, p. 163, Dec. 2017.
[18] Q. Song, X. Wang, T. Qiu, and Z. Ning, "An interference coordination-based distributed resource allocation scheme in heterogeneous cellular networks," *IEEE Access*, vol. 5, pp. 2152–2162, 2017.
[19] C. Yang, J. Li, Q. Ni, A. Anpalagan, and M. Guizani, "Interference-aware energy efficiency maximization in 5G ultra-dense networks," *IEEE Trans. Commun.*, vol. 65, no. 2, pp. 728–739, Feb. 2017.
[20] A. Virdis, G. Stea, D. Sabella, and M. Caretti, "A distributed power-saving framework for LTE HetNets exploiting almost blank subframes," *IEEE Trans. Green Commun. Netw.*, vol. 1, no. 3, pp. 235–252, Sep. 2017.
[21] Y. Liu, C. S. Chen, C. W. Sung, and C. Singh, "A game theoretic distributed algorithm for FeICIC optimization in LTE-A HetNets," *IEEE/ACM Trans. Netw.*, vol. 25, no. 6, pp. 3500–3513, Dec. 2017, doi: 10.1109/TNET.2017.2748567.
[22] S. Zou, N. Liu, Z. Pan, and X. You, "Joint power and resource allocation for non-uniform topologies in heterogeneous networks," in *Proc. IEEE 83rd Veh. Technol. Conf. (VTC Spring)*, Nanjing, China, May 2016, pp. 1–5.
[23] Y. Chen, X. Fang, and B. Huang, "Joint ABS power and resource allocations for eICIC in heterogeneous networks," in *Proc. 6th Int. Workshop Signal Des. Appl. Commun.*, Tokyo, Japan, Oct./Nov. 2013, pp. 92–95.
[24] W. Peng, M. Li, Y. Li, W. Gao, and T. Jiang, "Ultra-dense heterogeneous relay networks: A non-uniform traffic hotspot case," *IEEE Netw.*, vol. 31, no. 4, pp. 22–27, Jul./Aug. 2017.
[25] Q. Ye, B. Rong, Y. Chen, M. Al-Shalash, C. Caramanis, and J. G. Andrews, "User association for load balancing in heterogeneous cellular networks," *IEEE Trans. Wireless Commun.*, vol. 12, no. 6, pp. 2706–2716, Jun. 2013.
[26] M. Assaad, "Optimal fractional frequency reuse (FFR) in multicellular OFDMA system," in *Proc. IEEE 68th Veh. Technol. Conf. (VTC Fall)*, Calgary, BC, Canada, Sep. 2008, pp. 1822–1826.
[27] F. Alfarhan, R. Lerbour, and Y. L. Helloco, "An optimization framework for LTE eICIC and reduced power eICIC," in *Proc. IEEE Global Commun. Conf. (GLOBECOM)*, San Diego, CA, USA, Dec. 2015, pp. 1–6.
[28] S. Sadr, A. Anpalagan, and K. Raahemifar, "Radio resource allocation algorithms for the downlink of multiuser OFDM communication systems," *IEEE Commun. Surveys Tuts.*, vol. 11, no. 3, pp. 92–106, 3rd Quart., 2009.
[29] U. Feige, M. Feldman, and I. Talgam-Cohen, "Oblivious rounding and the integrality gap," in *Proc. LIPIcs Approximation, Randomization, Combinat. Optim. Algorithms Techn. (APPROX/RANDOM)*, Paris, France, Sep. 2016, pp. 1–23.
[30] D. P. Bertsekas, *Convex Optimization Theory*. Nashua, NH, USA: Athena Scientific, 2009.
[31] S. Boyd and L. Vandenberghe, *Convex Optimization*. New York, NY, USA: Cambridge Univ. Press, 2004.
[32] A. Bedekar and R. Agrawal, "Optimal muting and load balancing for eICIC," in *Proc. 11th Int. Symp. Workshops Modeling Optim. Mobile, Ad Hoc Wireless Netw. (WiOpt)*, Tsukuba, Japan, May 2013, pp. 280–287.
[33] K. Son, S. Chong, and G. Veciana, "Dynamic association for load balancing and interference avoidance in multi-cell networks," *IEEE Trans. Wireless Commun.*, vol. 8, no. 7, pp. 3566–3576, Jul. 2009.

[34] T. Nguyen and Y. Han, "A proportional fairness algorithm with QoS provision in downlink OFDMA systems," *IEEE Commun. Lett.*, vol. 10, no. 11, pp. 760–762, Dec. 2006.
[35] E. Chlamtac and M. Tulsiani, "Convex relaxations and integrality gaps," in *Handbook on Semidefinite, Conic and Polynomial Optimization*, M. F. Anjos and J. B. Lasserre, Eds. Boston, MA, USA: Springer, 2012, pp. 139–169.

JINJING HUANG received the B.S. degree in telecommunications engineering from the Shandong University of Science and Technology, Qingdao, China, in 2010. He is currently pursuing the Ph.D. degree with Xidian University under the supervision of Prof. J.-D. Li. His research interests focus on inter-cell interference coordination in LTE\LTE-A networks and interference management in heterogeneous cellular networks.

JIANDONG LI (M'01–SM'05) received the B.E., M.S., and Ph.D. degrees in communications engineering from Xidian University, Xi'an, China, in 1982, 1985, and 1991, respectively. He has been a Faculty Member of the School of Telecommunications Engineering, Xidian University since 1985, where he is currently a Professor and the Vice Director of the Academic Committee of the State Key Laboratory of Integrated Service Networks. He was a Visiting Professor with the Department of Electrical and Computer Engineering, Cornell University, Ithaca, NY, USA, from 2002 to 2003. His research interests include wireless communication theory, cognitive radio, and signal processing. He was a recipient of the Distinguished Young Researcher from NSFC and Changjiang Scholar from the Ministry of Education, China. He served as the General Vice Chair for ChinaCom 2009 and the TPC Chair of IEEE ICCC 2013.

ZICHEN CHEN received the B.E. degree in telecommunication engineering from Xidian University, Xi'an, China, in 2009, where he is currently pursuing the Ph.D. degree with the School of Telecommunications Engineering. His main research interests include heterogeneous network, massive MIMO, and distributed algorithms.

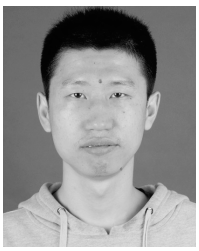

HAO PAN received the B.S. and M.S. degrees in communications engineering from Xidian University, Xi'an, China, 2008 and 2011, respectively, where he is currently pursuing the Ph.D. degree. His research interests include network coding and wireless communication.